



EGYPTIAN ACADEMIC JOURNAL OF  
**BIOLOGICAL SCIENCES**  
TOXICOLOGY & PEST CONTROL

F



ISSN  
2090-0791

WWW.EAJBS.EG.NET

**Vol. 16 No. 2 (2024)**

[www.eajbs.eg.net](http://www.eajbs.eg.net)



## Insight on Therapeutic Effect of Ultrasound Nanobubbles Loaded with TAK-242 on Aflatoxin B1 induced Hepatorenal Toxicity in Rats

Sahar M. Abo El Wafa<sup>1</sup>, Sania K. Elwia<sup>2\*</sup>, Sally Elsharkawey<sup>1</sup>

<sup>1</sup>Forensic Medicine and Clinical Toxicology Department, Faculty of Medicine, Benha University, Benha, Egypt.

<sup>2</sup>Medical Biochemistry and Molecular Biology Department, Faculty of Medicine, Benha University, Benha, Egypt.

\*Email: [Sanya.khairy@gmail.com](mailto:Sanya.khairy@gmail.com)

### REVIEWINFO

#### Review History

Received:13/7/2024

Accepted:23/9/2024

Available:27/9/2024

#### Keywords:

Ultrasound,  
Nanobubbles,  
TAK-242,  
Aflatoxin B1,  
TLR4, NGAL.

### ABSTRACT

Aflatoxin B1 (AFB1) is acknowledged as a remarkably powerful genotoxic and hepatocarcinogenic substance, posing a significant public health risk. This study examined the capacity of ultrasound nanobubbles containing TAK-242 to alleviate hepatorenal toxicity induced by AFB1 in rats. A total of thirty-two male albino rats were divided into four equal groups: a control group, a group treated with TAK-242-loaded nanobubbles, a group exposed to AFB1, and a group receiving both AFB1 and TAK-242-loaded nanobubbles. The therapeutic intervention involved the administration of 150  $\mu$ l of nanobubbles twice a day after exposure to AFB1, together with a 15-minute ultrasound session at a frequency of 5 MHz. Following a 14-day duration, evaluations were conducted using biochemical analyses, gene expression investigations, and histological evaluations. Rats that were intoxicated with AFB1 showed decreased levels of glutathione (GSH), superoxide dismutase (SOD), and catalase (CAT) in their plasma. Additionally, they exhibited increased levels of malondialdehyde (MDA), interleukin-6 (IL-6), tumor necrosis factor-alpha (TNF $\alpha$ ), alanine aminotransferase (ALT), aspartate aminotransferase (AST), alkaline phosphatase (ALP), urea, and creatinine. In addition, there was an increase in the expression of toll-like receptor 4 (TLR4) and neutrophil gelatinase-associated lipocalin (NGAL) genes, along with significant histopathological damage to the liver and kidney tissues. The administration of TAK-242-loaded nanobubbles significantly improved these harmful effects, by strengthening the body's antioxidant defenses and decreasing both the biochemical and histopathological changes in the liver and kidney tissues.

### INTRODUCTION

Aflatoxins, a group of secondary metabolites, are biosynthesized by the fungal species *Aspergillus flavus* and *Aspergillus parasiticus* within various feed matrices. Aflatoxin B1 (AFB1), a preeminent member of this mycotoxin family, exhibits profound genotoxic and hepatocarcinogenic potential. (Li *et al.*, 2018). The aflatoxin mycotoxins encompass a spectrum of variants: *A. flavus* is responsible for the exclusive production of aflatoxins B1 and B2, while *A. parasiticus* synthesizes aflatoxins B1, B2, G1, and G2. Among these, AFB1 is notably the most ubiquitous and is distinguished by its heightened toxicity in humans and

its significant carcinogenicity in laboratory animals that are predisposed to such effects (Mtimet *et al.*, 2015). Regions characterized by warm, humid climates coupled with abundant rainfall create ideal conditions for the proliferation of these molds. Suboptimal food storage practices facilitate the contamination of AFB1, with staples such as peanuts, corn, rice, milk, and oil being particularly vulnerable (Medina *et al.*, 2014). Once foodstuffs are tainted with AFB1, their removal becomes exceedingly challenging. (Rushing and Selim, 2019). The insidious nature of AFB1 exposure, often undetected, can lead to the development of hepatocellular carcinoma over an extended period (Nugraha *et al.*, 2018).

The liver and kidneys are the main organs of focus in numerous studies due to their vital functions in metabolism, detoxification, and elimination of foreign substances, which makes them especially susceptible to the overall harmful effects of AFB1. (Frag and Alagawany, 2018). Consequently, it is imperative to devise efficient approaches to alleviate the hepatorenal toxicity caused by AFB1. (Deng *et al.*, 2020).

Ultrasonic nanobubble-based drug delivery systems have garnered considerable research interest due to their tiny size, exceptional stability, and unique physical and surface properties. These characteristics facilitate efficient passage across the vascular endothelium and penetration into target tissues (Suzuki *et al.*, 2016, Endo-Takahashi and Negishi, 2020, Sun *et al.*, 2020). This therapeutic modality leverages the administration of nanobubbles conjugated with pharmacological agents or genetic material, followed by the application of ultrasound irradiation, which markedly enhances the absorption rate of these therapeutics within the targeted region (Chen *et al.*, 2014).

Toll-like receptors (TLRs) are an essential group of receptors that play a fundamental role in the body's main defense system against microbial organisms. The receptors have the ability to detect both harmful exterior pathogens and internal signals from dying cells and injured tissues. This allows them to coordinate the important interaction between the innate and adaptive immune responses (El-Zayat *et al.*, 2019).

TLRs are essential regulators of the inflammatory response and are involved in multiple cellular processes that are triggered during episodes of acute kidney damage. Consequently, numerous anti-inflammatory substances that specifically target TLRs have been investigated in preclinical research to alleviate renal damage linked to acute kidney injury. (Vázquez-Carballo *et al.*, 2021). TLRs detect molecules derived from microbes, and when they are activated, they initiate the NF- $\kappa$ B pathway, which results in a series of pro-inflammatory reactions. (Shah *et al.*, 2013).

As a consequence of hepatic injury, patients frequently exhibit endotoxemia and elevated plasma concentrations of inflammatory cytokines. The activation of TLRs emerges as a pivotal molecular mechanism that is closely associated with disease progression. (Kawai and Akira, 2010). Excessive, uncontrolled, or sustained activation of TLRs can lead to a chronic inflammatory state, contributing to the development of various immune-mediated pathologies. Thus, strict regulation of the TLR4 signaling pathway is essential to protect the host from excessive inflammatory responses (Vázquez-Carballo *et al.*, 2021).

TAK-242 is a small-molecule inhibitor that mitigates the release of inflammatory cytokines induced by pathogens through the inhibition of TLR-4-mediated signaling pathways. Additionally, it exhibits inhibitory effects on the production of NO and TNF- $\alpha$  triggered by the TLR4-specific ligand lipopolysaccharide (LPS) (Kawamoto *et al.*, 2008). TAK-242's restorative properties against TLR4-associated inflammatory responses contribute to the reduction of mitochondrial component damage and hepatocyte necrosis, while concurrently improving hepatic function (Zhong *et al.*, 2019).

TAK-242, a small-molecule inhibitor, specifically hinders TLR4 activation by attaching to the intracellular residue Cys747. Having established safety in human investigations, TAK-242 is under clinical development as a potential treatment drug for sepsis.

Additionally, it has been found to minimize target organ damage and systemic inflammation in animal models (Behzadi *et al.*, 2022). TAK-242 achieves its selective inhibition by interfering with the interactions between TLR4 and its adaptor molecules, toll/interleukin-1 receptor domain-containing adaptor protein (TIRAP), and toll/interleukin-1 receptor domain-containing adaptor protein inducing interferon- $\beta$ -related adaptor molecule (TRAM) (Matsunaga *et al.*, 2011).

Neutrophil gelatinase-associated lipocalin (NGAL), a protein weighing 25 kilodaltons, is quickly increased in renal tissue as a result of ischemia events and tubular injury (Batte *et al.*, 2022). NGAL functions as a biomarker, being released by neutrophils in the innate immune system in response to inflammatory processes and renal ischemia (Zhang *et al.*, 2018).

Aflatoxin presents a substantial public health risk because of its carcinogenic characteristics and its contamination of food items, which has a negative impact on consumer well-being. There is a significant absence of studies examining the potential of ultrasound nanobubbles loaded with TAK-242 to improve aflatoxin B1-induced hepatorenal damage. This study seeks to assess the potential of ultrasound nanobubbles loaded with TAK-242 to act as a therapy and alleviate the hepatorenal toxic effects caused by aflatoxin B1 in rats. This examination will specifically examine blood markers of liver and kidney function, markers of oxidative stress, gene expression of TLR4 and NGAL, and histological alterations in liver and kidney tissues

## MATERIALS AND METHODS

### Chemicals and Drugs:

- Aflatoxin B1 was purchased from Sigma Chemical Co. (St. Louis, MO, USA).
- Kits for assaying ALT, AST, CAT, SOD, reduced glutathione (GSH), MDA, IL-6 and TNF- $\alpha$  were obtained from Biodiagnostic Company (29 El-Tahrir St. Dokki, Giza, Egypt).
- TAK-242, obtained from sigma-Aldrisch chemical co lots Missouri, USA.
- All the other chemicals and reagents were of analytical grades.

### Animals:

A total of thirty-two adult male Sprague-Dawley rats, ranging in age from 2 to 3 months and weighing between 180 and 220 grams, were acquired from the Experimental Animal Breeding Farm located in Helwan, Cairo. The rats were kept in groups of eight per cage in a well-ventilated setting at the ambient room temperature in the Pharmacology Department of Benha Faculty of Medicine. A 14-day acclimation period was given, during which the rats were allowed to freely consume water and regular chow, following a 12-hour light/12-hour dark cycle. The administration of the dose was consistently scheduled for 12 P.M. The experimental procedures followed the ethical rules of the Benha Faculty of Medicine to ensure the humane treatment of animals. Measures were taken to minimize the number of animals utilized and to alleviate their pain.

### Experimental Design:

The rats were assigned at random to four groups of equal size and exposed to a treatment regimen consisting of aflatoxin B1 and TAK-242-loaded nanobubbles for 14 consecutive days, according to the following protocol:

**Group I (Control group)** was provided with a regular basal diet.

**Group II:** Each rat was administered a 150  $\mu$ l intravenous injection of nanobubbles loaded - TAK-242 (3 mg/kg) into the tail vein, the procedure was performed bi-daily, utilizing ultrasonic irradiation at a frequency of 5 MHz and a mechanical index (MI) of 1.2 for a duration of 15 minutes per session (Engelmann *et al.*, 2020).

**Group III:** Administered a basal diet supplemented with AFB1 (3 mg/kg) for a period of 14 consecutive days (Abdel-Wahhab *et al.*, 2007).

**Group IV:** Subjects were administered a basal diet containing AFB1 at a concentration of 3 mg/kg. Additionally, they received intravenous injections of 150  $\mu$  nanobubbles loaded with TAK-242 at a dosage of 3 mg/kg. The injections were initiated within 22 hours after the consumption of AFB1. The treatment was given on alternate days, along with ultrasonic exposure at a frequency of 5 MHz and an intensity of 1.2 mechanical index (MI), for a duration of 15 minutes per session. Following a period of 14 consecutive days, the rats were euthanized in order to conduct additional analysis.

#### **Blood and Tissue Sampling:**

At the conclusion of the experimental protocol, blood samples were collected from the tail veins of the rats. These samples were allowed to clot at room temperature for 30 minutes and were subsequently centrifuged at 2500 rpm for 15 minutes. The separated sera were stored at -20°C until biochemical analysis of ALT, and AST They were estimated spectrophotometrically using commercial test kits of (AST and ALT) supplied by Diamond Diagnostics. The level of both (AST and ALT) was expressed as (U/L), CAT, SOD, reduced glutathione (GSH), MDA was measured using a colorimetric method (Bio diagnostics, Dokki, Giza, Egypt), IL-6 and TNF- $\alpha$  were estimated by enzyme-linked immunosorbent assay (ELISA Rat TNF- $\alpha$  and caspase-3 Immunoassay kits) manufactured by Orgenium, Helsinki, USA. Their levels were expressed as (pg/ml). Were determined using the colorimetric method according to the manufacturer's instructions.

Following these procedures, the rats were euthanized by decapitation. Liver and kidney tissues were then harvested and rinsed with normal physiological saline solution for subsequent histopathological examination.

#### **TAK-242 preparation**

<b>Synonyms</b>	TLR4 Inhibitor, TAK-242 InSolution, Ethyl-(6R)-6-(N-(2-chloro-4-fluorophenyl)sulfamoyl)cyclohex-1-ene-1-carboxylate, (R)-Ethyl 6-(N-(2-chloro-4-fluorophenyl)sulfamoyl)cyclohex-1-enecarboxylate
<b>Description</b>	A cell-permeable cyclohexenecarboxylate that disrupts TLR4 interaction with adaptor molecules TIRAP and TRAM by selectively binding to TLR4, but not TLR1-3 or TLR5-10, via TLR4 intracellular Cys747 residue. Shown to effectively inhibit TLR4-mediated signaling events, including LPS-induced NO and inflammatory cytokines production in murine RAW264.7 macrophages (IC <sub>50</sub> = 1.8, 1.3, and 1.9 nM, respectively, against NO, IL-6, and TNF- $\alpha$ production), TLR4/TIRAP-dependent NF- $\kappa$ B activity as well as TLR4/TIRAP- and TLR4/TRAM-dependent ISRE activity (IC <sub>50</sub> < 300 nM) in HEK293-hTLR4/MD2-CD14 transfected with either TIRAP or TRAM. When administered at an i.v. A dose of 3 mg/kg, TAK-242 is reported to completely prevent LPS- (7 mg/kg, i.p.) induced death in mice <i>in vivo</i> . Complete elimination of septic shock-induced death can be extended to live <i>E. coli</i> -infected mice when co-administered with ceftazidime (3 mg/kg TAK-242 and 20 mg/kg ceftazidime, i.v.).
<b>Form</b>	Liquid
<b>Formulation</b>	A 25 mM (2 mg/221 $\mu$ L) sterile-filtered solution of TLR4 Inhibitor, TAK-242 (Cat. No. 614316) in DMSO.
<b>Intert gas (Yes/No)</b>	Packaged under inert gas

<b>CAS number</b>	243984-11-4		
<b>Chemical formula</b>	C <sub>15</sub> H <sub>17</sub> ClFNO <sub>4</sub> S		
<b>Purity</b>	≥98% by HPLC		
<b>Storage</b>	Protect Avoid ≤ Hygroscopic	from	light freeze/thaw -70°C

It was purchased from Sigma-Aldrich In Solution™ TLR4 Inhibitor, TAK-242 - CAS 243984-11-4 – Calbiochem (Matsunaga *et al.*, 2011).

TAK-242 was dissolved in DMSO and then diluted in sterile endotoxin-free water. The final concentration of DMSO was 1%. The dissolved TAK-242 (1%) was injected in the tail vein (3 mg/kg body weight) A typical nanobubble (NB) sample is anticipated to consist of a combination of gas-filled bubbles and aqueous-filled liposomes that are around the same size.

#### **NBs Preparation:**

Nanobubbles were created by combining DPPC (1,2-dipalmitoyl-sn-glycero-3-phosphocholine) and DPSE-PEG2000 (1,2-distearoyl-sn-glycero-3-phosphoethanolamine-N-[methoxy (polyethylene glycol)-2000]) lipids in a ratio of 95:5. The resulting lipid concentration was 2 mg/mL, using Avanti Polar Lipids, located in AL, USA. The lipids were initially dissolved in a combination of chloroform and methanol in equal proportions. The solvents were then removed through evaporation using nitrogen gas. Subsequently, the lipids were rehydrated in a solution of PBS (phosphate-buffered saline) containing 1% (volume/volume) glycerol. The lipid solution was emulsified with C4F10 (perfluorobutane) gas using a multiplexed microspray microfluidic system to create bubbles, following the method reported by Peyman *et al.* (Peyman *et al.*, 2016).

#### **NB with Liposome Loaded with TAK242:**

The lipid blend consisting of DSPC (1,2-distearoyl-sn-glycero-3-phosphocholine), cholesterol, and DSPE-PEG2000 was dehydrated in round-bottom flasks under a nitrogen atmosphere. The molar ratio of the lipids was maintained at 63:32:5, resulting in a total lipid content of 15 mg/mL. The lipid film obtained was subsequently reconstituted either in phosphate-buffered saline (PBS) to create liposomes or in a stock solution of NB for Nested-NB synthesis. The rehydration process involved stirring for one hour. In order to administer TAK-242, the chemical (Millipore) was dissolved in a solution containing 1% DMSO and 0.9% saline, resulting in a concentration of 0.4 mg/mL. This solution was then administered via the tail vein. Prior to the rehydration stage, TAK-242 was added to the lipid mixture at a final concentration of 100 mM. The rehydrated lipid solution was homogenized by extrusion via a 400 nm PTFE membrane. TAK-242 and NBs without capsules were separated by centrifugation at 17,000g for 20 minutes and then washed with PBS. The centrifugation and washing procedure was repeated once more (Feng *et al.*, 2023, Tian *et al.*, 2018).

#### **Stability of the Nanobubbles:**

The synthesized nanobubbles exhibited robust stability at temperatures of 25 °C and 37 °C when diluted in both plasma and saline solutions, a finding confirmed through photo correlation spectroscopy analyses. It was determined that the mean diameter of the nanobubbles remained consistent at 25 °C after incubation in plasma. Conversely, at 37 °C, an enhancement in nanobubble stability was observed over time, as indicated by an increase in their mean diameter (Zhang *et al.*, 2020).

**Ultrasound Exposure:**

The rats were anesthetized using isoflurane inhalation (Ifran Liq.®, HanaPharm, Gyeonggi-do, Korea) and placed on the operating table. Experimental conditions were rigorously controlled at a temperature of 37°C (Ani1400T-TC, LMSKorea, Gyeonggi-do, Korea). The rats' limbs were immobilized to maintain proper positioning, while an ultrasound device (F37®, Hitachi Aloka Medical, Tokyo, Japan) was employed to precisely locate the liver and kidney. The ultrasonic probe was secured in a fixed position to ensure stability during the experiment. Ultrasound irradiation was then administered according to the designated experimental protocol. Fluorescence imaging was captured at absorption and emission wavelengths of 470 nm and 540 nm, respectively (Park and Park, 2023).

**Sampling:**

Blood samples were collected from the tail veins of the rats. Blood samples were stored at -80° for further investigation.

**RNA Extraction:**

RNA was isolated from blood samples using the RNeasy RNA extraction kit (Qiagen, USA), following the manufacturer's instructions. The quantity of the eluted RNA was measured using the NanoDrop 2000 spectrophotometer (Thermo Fisher, USA).

**cDNA Synthesis and PCR Amplification:**

The One-Step RT-PCR Kit with SYBR® Green (BioRad, USA) was utilized following the manufacturer's recommended protocols. The SYBR green-based RT-PCR assay was carried out using a sequence detection system provided by Bio-Rad Laboratories Inc. (Hercules, CA, USA).

Real-time RT-PCR was performed for 10 minutes at 50°C and for 5 minutes at 95°C. Thirty PCR cycles of denaturation for 10 seconds at 95°C and annealing with extension for 30 seconds at 60°C were then conducted. 7900HT Fast real time PCR system (Rotorgene)

Quantitative gene expression analysis of TLR4 and NGAL was performed employing the 2- $\Delta\Delta$ CT method, with GAPDH as the reference housekeeping gene (Table 1).

**Table 1:** Primer sequence of TLR4, NGAL and GAPDH

Gene	Sequence
TLR4 Sense: 5'- ACCTGGCTGGTTTACACGTC-3'	Antisense: 5'- CTGCCAGAGACATTGCAGAA-3'
NGAL neutrophil gelatinase-associated lipocalin 5- CACCACGGACTACAACCAGTTCGC-3	5- TCAGTTGTCAATGCATTGGTCGGTG- 3
GAPDH 50- ACCACAGTCCATGCCATCAC-30 65	5-CACCACCCTGTTGCTGTAGCC-30

**Histopathological study:**

Each rat in all experimental groups had their liver and kidney tissue specimens collected and then fixed in 10% neutral-buffered formalin for 48 hours. Subsequently, the specimens were treated using the paraffin embedding procedure. Hepatic and renal tissue sections underwent staining with hematoxylin and eosin (H&E), using the methodology outlined by Bancroft and Gamble (Bancroft and Gamble, 2008), and were thoroughly scrutinized for any histopathological changes.

**Statistical Analysis:**

The results were collected, organized, and presented as the average value plus or minus the measure of variability. The study utilized a one-way analysis of variance

(ANOVA) to assess the disparities in average values between the treatment and control groups. The statistical software SPSS version 16 was employed for this purpose. A P value of less than 0.05 was regarded as indicative of statistical significance.

## RESULTS

The contemporaneous delivery of ultrasonic nanobubbles loaded with TAK-242 had a modulatory effect on the oxidative stress generated by AFB1 exposure, as shown in Table 2. The group exposed to AFB1 showed a substantial reduction ( $p < 0.05$ ) in plasma levels of glutathione (GSH), superoxide dismutase (SOD), and catalase (CAT), as well as a significant increase ( $p < 0.05$ ) in plasma malondialdehyde (MDA) levels compared to the control group. Conversely, when TAK-242-loaded ultrasonic nanobubbles were administered simultaneously with AFB1, there was a substantial and statistically significant rise in plasma levels of GSH, SOD, and CAT, and a significant drop ( $p < 0.05$ ) in plasma levels of MDA, as compared to the AFB1 group.

**Table 2:** Statistical comparison between all studied groups regarding MDA, GSH, SOD and Catalase by ANOVA test.

	Group (I) Control group	Group (II) US nanobubbles loaded with TAK-242 group	Group (III) Aflatoxin B1 group	Group (IV) Aflatoxin B1 + US nanobubbles loaded with TAK- 242group	P value
MDA (nmol/ml)	2.53±0.23 <sup>^€*</sup>	2.27±0.24 <sup>€*</sup>	5.75± 0.22 <sup>\$ ^*</sup>	4.24± 0.20 <sup>\$^€</sup>	0.000**
GSH (µm/ml)	0.56±0.03 <sup>^€*</sup>	0.44±0.01 <sup>€*</sup>	0.22±0.02 <sup>\$ ^*</sup>	0.31±0.01 <sup>\$^€</sup>	0.000**
SOD (µ/ml)	354±2.56 <sup>^€*</sup>	310±13.09 <sup>€*</sup>	243±2.56 <sup>\$ ^*</sup>	263±3.20 <sup>\$^€</sup>	0.000**
Catalase (µ /ml)	8.51 ± 0.31 <sup>^€*</sup>	6.54±0.29 <sup>€*</sup>	4.64± 0.26 <sup>\$ ^*</sup>	5.35± 0.27 <sup>\$^€</sup>	0.000**

All values are expressed as mean±SD

Number of rats in each group = 8

The mean difference is significant at  $< 0.05$  level.

highly significant(\*\*)

\$: indicate significant change as compared with a group (I)

^: indicate significant change as compared with a group (II)

€: indicate significant change as compared with a group (III)

\*: indicate significant change as compared with a group (IV)

Table 3, shows that AFB1 intoxication resulted in a substantial and statistically significant elevation ( $p < 0.05$ ) of IL-6 and TNF- $\alpha$  levels in comparison to the control group. In contrast, when TAK-242-loaded ultrasonic nanobubbles were administered at the same time as AFB1, there was a substantial and statistically significant reduction ( $p < 0.05$ ) in the levels of these cytokines compared to the group that only received AFB1.

Table 4, demonstrates that AFB1 intoxication resulted in a statistically significant elevation ( $p < 0.05$ ) in liver function tests (ALT, AST, ALP) and kidney function tests (urea and creatinine) as compared to the control group. Conversely, when TAK-242-loaded ultrasonic nanobubbles were administered at the same time as AFB1, there was a substantial and statistically significant reduction ( $p < 0.05$ ) in the levels of AFB1 compared to the group that only received AFB1.

**Table 3:** Statistical comparison between all studied groups regarding TNF $\alpha$ , IL6 by ANOVA test Table.

	Group (I) Control group	Group (II) US nanobubbles loaded with TAK-242 group	Group (III) Aflatoxin B1 group	Group (IV) Aflatoxin B1 + US nanobubbles loaded with TAK-242 group	P value
<b>TNF<math>\alpha</math></b> (pg/ml)	37.74 $\pm$ 0.34 $\wedge$ $\epsilon$ *	35.69 $\pm$ 0.32 \$ $\epsilon$ *	77.65 $\pm$ 0.24 \$ $\wedge$ *	48.83 $\pm$ 3.71 \$ $\wedge$ $\epsilon$	0.000**
<b>IL6</b> (Pg/ml)	7.46 $\pm$ 0.27 $\wedge$ $\epsilon$ *	6.53 $\pm$ 0.19\$ $\epsilon$ *	15.88 $\pm$ 0.05 \$ $\wedge$ *	9.61 $\pm$ 0.15 \$ $\wedge$ $\epsilon$	0.000**

All values are expressed as mean $\pm$ SD

Number of rats in each group = 8

The mean difference is significant at < 0.05 level.

highly significant(\*\*)

\$: indicate significant change as compared with a group (I)

$\wedge$ : indicate significant change as compared with a group (II)

$\epsilon$ : indicate significant change as compared with a group (III)

\*: indicate significant change as compared with a group (IV)

**Table 4:** Statistical comparison between all studied groups regarding liver and kidney functions test by ANOVA test.

	Group (I) Control group	Group (II) US nanobubbles loaded with TAK-242 group	Group (III) Aflatoxin B1 group	Group (IV) Aflatoxin B1 + US nanobubbles loaded with TAK-242 group	P value
<b>AST</b> ( $\mu$ /L)	27.45 $\pm$ 0.57 $\wedge$ $\epsilon$ *	25.74 $\pm$ 0.22 \$ $\epsilon$ *	86.62 $\pm$ 0.28 \$ $\wedge$ *	36.84 $\pm$ 0.17 \$ $\wedge$ $\epsilon$	0.000**
<b>ALT</b> ( $\mu$ /L)	16.73 $\pm$ 0.24 $\wedge$ $\epsilon$ *	15.80 $\pm$ 0.65 \$ $\epsilon$ *	55.85 $\pm$ 0.11\$ $\wedge$ *	20.73 $\pm$ 0.16 \$ $\wedge$ $\epsilon$	0.000**
<b>ALP</b> ( $\mu$ /L)	30.54 $\pm$ 0.43 $\wedge$ $\epsilon$ *	28.71 $\pm$ 0.23 \$ $\epsilon$ *	89.59 $\pm$ 0.22 \$ $\wedge$ *	35.87 $\pm$ 0.09 \$ $\wedge$ $\epsilon$	0.000**
<b>Urea</b> (mg /dl)	28.59 $\pm$ 0.26 $\wedge$ $\epsilon$ *	26.72 $\pm$ 0.28 \$ $\epsilon$ *	65.32 $\pm$ 0.28 \$ $\wedge$ *	40.24 $\pm$ 0.55 \$ $\wedge$ $\epsilon$	0.000**
<b>Creatinine</b> (mg/dl)	0.33 $\pm$ 0.02 $\epsilon$ *	0.31 $\pm$ 0.01 $\epsilon$ *	3.7 $\pm$ 0.32 \$ $\wedge$ *	0.8 $\pm$ 0.09 \$ $\wedge$ $\epsilon$	0.000**

All values are expressed as mean $\pm$ SD

Number of rats in each group = 8

The mean difference is significant at < 0.05 level.

highly significant(\*\*)

\$: indicate significant change as compared with a group (I)

$\wedge$ : indicate significant change as compared with a group (II)

$\epsilon$ : indicate significant change as compared with a group (III)

\*: indicate significant change as compared with a group (IV)

Table 5, clearly shows that AFB1 intoxication led to a substantial increase ( $p < 0.05$ ) in the expression of TLR4 and NGAL genes, compared to the control group. Concurrently administering TAK-242-loaded ultrasonic nanobubbles with AFB1 resulted in a substantial decrease ( $p < 0.05$ ) in the expression of TLR4 and NGAL genes compared to the AFB1 group.

**Table 5:** Statistical comparison between all studied groups regarding TLR4 and NGAL by ANOVA test.

	Group (I) Control group	Group (II) US nanobubbles loaded with TAK-242 group	Group (III) Aflatoxin B1 group	Group (IV) Aflatoxin B1 + US nanobubbles loaded with TAK-242group	P value
TLR4	1€	1 €	5.67±.83 \$ ^*	1.17± 0.78 €	< 0.001**
NGAL	1€	1 €	6.19±0.87\$ ^*	1.9±0.7 €	< 0.001**

All values are expressed as mean±SD

Number of rats in each group = 8

The mean difference is significant at < 0.05 level.

highly significant(\*\*)

\$: indicate significant change as compared with a group (I)

^: indicate significant change as compared with a group (II)

€: indicate significant change as compared with a group (III)

\*: indicate significant change as compared with a group (IV)

In regards to the histopathological analysis, liver tissue samples stained with H&E revealed a normal histological structure in the control group. This was observed as a central vein with strands of hepatocytes extending from it towards the outer edges, with normal sinusoids separating them (Fig. 1A). The rats that received TAK-242-loaded ultrasonic nanobubbles exhibited hepatic histoarchitecture that was very similar to normal (Fig. 1B). The liver tissue of rats exposed to AFB1 exhibited a congested central vein, hydropic degeneration, necrosis, and inflammatory foci, as depicted in Figure 1C. In the group that received both TAK-242-loaded ultrasonic nanobubbles and AFB1 at the same time, there was a noticeable improvement in the structure of the liver tissue and a return to normal histomorphological features, with the exception of some hydropic degeneration and a congested central vein (Fig. 1D).

Microscopic images of rat kidneys from the control group, stained with hematoxylin and eosin (H&E), revealed typical renal anatomy with a large number of glomeruli (Fig. 2A). The rats who received TAK-242-loaded ultrasonic nanobubbles exhibited glomeruli and tubules that were almost normal, as seen in Figure 2B. The kidney tissue of rats exposed to AFB1 exhibited congestion, hydropic degeneration, and necrosis foci, as depicted in Figure 2C. The group that received both TAK-242-loaded ultrasonic nanobubbles and AFB1 showed improvement in the structure of the kidneys and a return to normal histomorphological features, with the exception of minor congestion and hydropic degeneration (Fig. 2D).

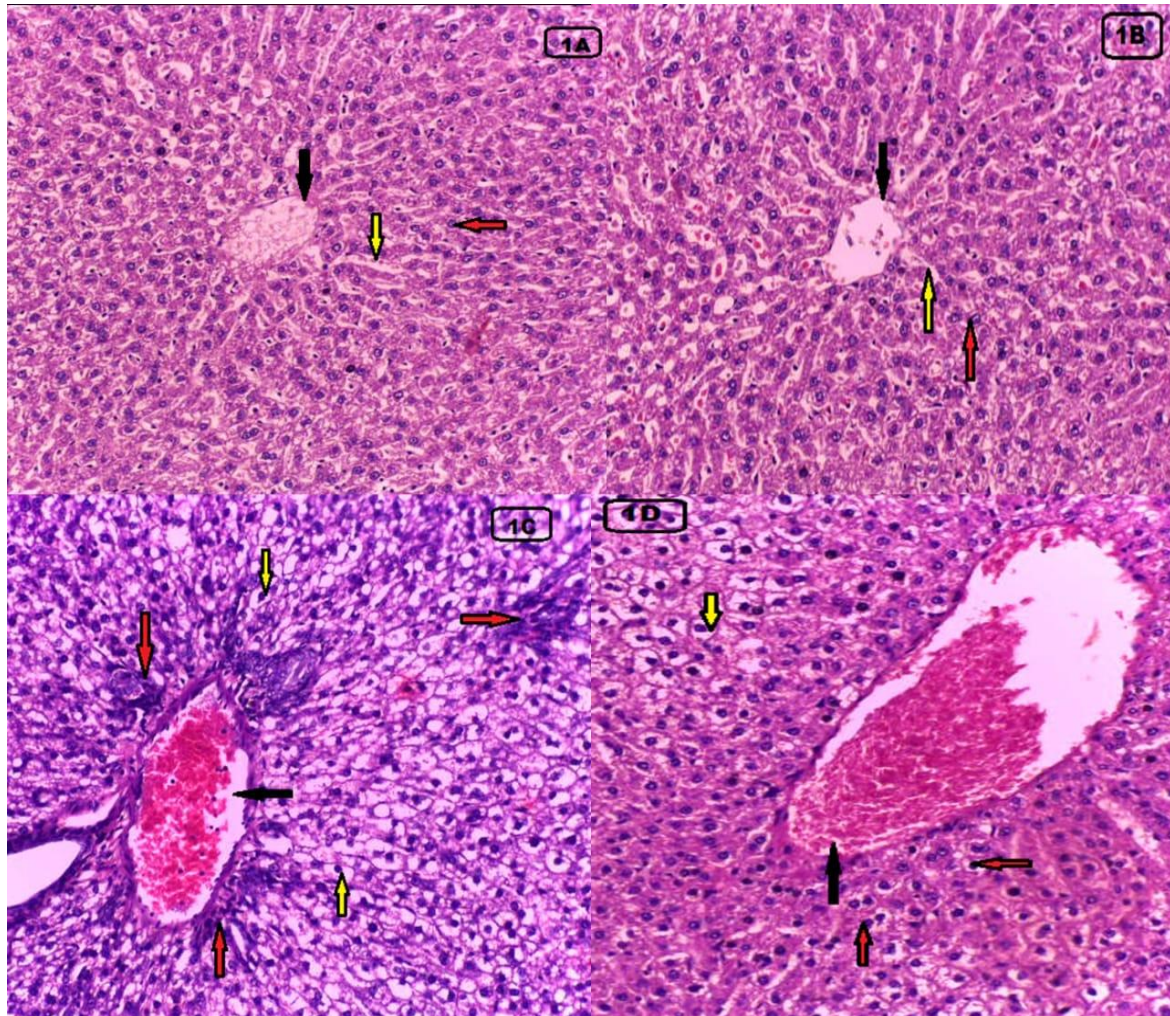


**Fig. 1:** (A) the control group showed liver tissue section with normal hepatic histological structure observed as normal central vein (black arrow) with normal strands of hepatocytes radiating from central vein to the periphery (red arrow) separated by normal sinusoids (yellow arrow) (H&E x20); (B) rats of US nanobubbles loaded with TAK-242 treated group showed near normal hepatic histoarchitecture (H&E x20); (C) liver of AFB1 exposed rats showed congested central vein (black arrow), hydropic degeneration (yellow arrow), necrosis and inflammatory foci (red arrow) (H&E x40); (D) rats of concurrent use of US nanobubbles loaded with TAK-242 with aflatoxin B1 treated group showed improvement in the hepatic histoarchitecture and restored normal histomorphological structures except from some hydropic degeneration (yellow arrow) and congested central vein (black arrow) (H&E x40).

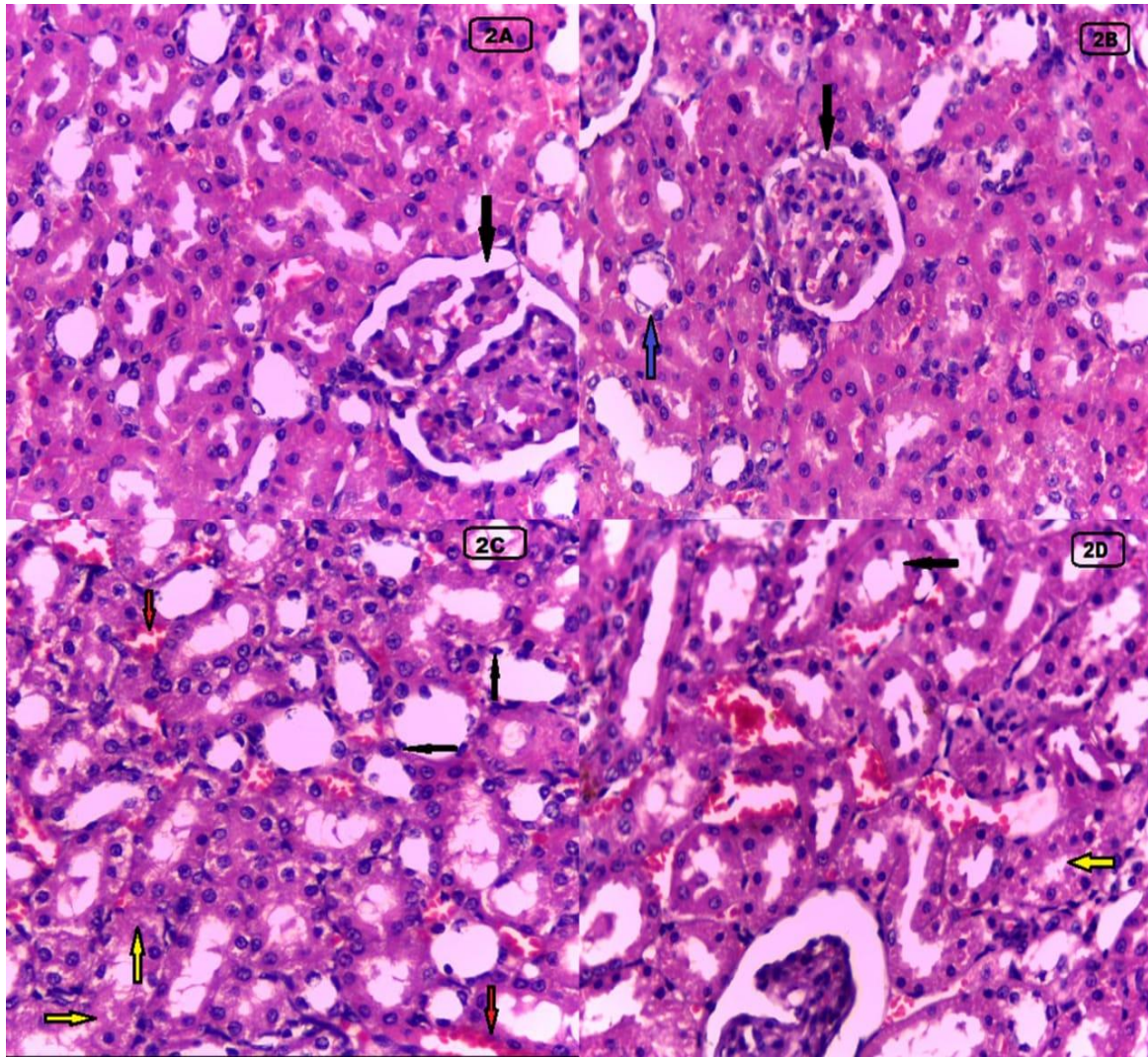


**Fig. 2:** (A) photomicrographs of rats' kidneys from control group stained with H&E showed normal renal structure with numerous glomeruli (black arrow) (H&E x40); (B) rats of US nanobubbles loaded with TAK-242 treated group showed near normal glomeruli (black arrow) and tubules (blue arrow) (H&E x40); (C) kidney of AFB1 exposed rats showed congestion (red arrow), hydropic degeneration (yellow arrow) and necrosis foci (black arrow) (H&E x40); (D) rats of concurrent use of US nanobubbles loaded with TAK-242 with aflatoxin B1 treated group showed improvement in the renal histoarchitecture and restored normal histomorphological structures (black arrow) except from some congestion and hydropic degeneration (yellow arrow) (H&E x40).

## DISCUSSION

Aflatoxins (AFs) are poisonous byproducts created by fungi that contaminate various feed products, posing a health risk to both humans and animals (Reda *et al.*, 2020, Somorin *et al.*, 2012). AFB1 is the predominant and very poisonous form among these metabolites (Rushing and Selim, 2019). The study found that exposure to AFB1 resulted in a notable rise in serum MDA levels and a considerable decline in the activities of GSH, SOD, and catalase. The reason for this is most likely the production of reactive oxygen species (ROS) as a result of the oxidation of AFs to their reactive intermediate (8,9-epoxide) by hepatic cytochrome P450 enzymes. The decrease in GSH levels can be due to its combination with aflatoxin

epoxide (Bernabucci *et al.*, 2011). GSH plays a crucial role in removing and combining free radicals and H<sub>2</sub>O<sub>2</sub> generated by harmful substances (Abdel-Aziem *et al.*, 2014).

The analysis revealed that AFB1-induced hepatorenal toxicity was demonstrated by a notable elevation in TNF- $\alpha$  and IL-6 activity, which aligns with previous findings of AFB1-induced liver damage (Aborehab and Waly, 2019). AFB1 triggers oxidative stress, resulting in harm to liver cells, programmed cell death, and the oxidation of lipids. This process alters the permeability of cell membranes and stimulates the release of cytokines (Lawrence, 2009). AFB1 also stimulates the production of cytokines, such as IL-6 and TNF- $\alpha$ , which play a role in promoting inflammation by interacting with their specific receptors (Hendrayani *et al.*, 2016).

The current investigation found that exposure to AFB1 significantly elevated the serum levels of ALT, ASP, ALP, urea, and creatinine. ALT, ASP, and ALP are biomarkers that are highly responsive to hepatic diseases, cirrhosis, and liver tissue necrosis. Elevated levels of ALT and ASP serve as early indicators of hepatocellular damage (Embaby *et al.*, 2015). The results align with the study conducted by Darwish *et al.* (Darwish *et al.*, 2011), which reported a substantial increase in ALT, ASP, creatinine, and uric acid levels in the blood serum when aflatoxins were introduced into animal diet. The variations in these biochemical parameters were particularly noticeable. The biochemical alterations observed suggest that there is an early insult to the liver cells after treatment with AFB1 (Choi *et al.*, 2010). Additionally, these changes emphasize that the kidney is a primary target of AFs and their metabolic byproducts (Li *et al.*, 2018). Sun *et al.* have also confirmed the harmful impact of AFs on liver and kidney functioning (Sun *et al.*, 2015).

Nanobubbles (NBs) are a new type of nanocarriers that respond to ultrasound and are specifically intended to improve the effectiveness of drug administration. These nanoparticles have the ability to move from blood arteries into nearby tissues, which enhances the effectiveness of delivering drugs and targeting specific areas. They demonstrate exceptional stability, superior encapsulation and drug loading efficiency, and enable an accelerated drug release rate when facilitated by ultrasound (Guo *et al.*, 2020).

The capillary walls are physically damaged due to the resonance of microbubbles when exposed to ultrasonic waves. This resonance causes the microbubbles to undergo cyclic size changes, leading to their eventual disintegration. This method is based on the assumption that ultrasonic radiation leads to the fragmentation of microbubbles into smaller particles, which in turn enhances the penetration of medicines or genes into tissue. Moreover, the presence of microbubbles in the bloodstream is disturbed by focused ultrasonic radiation, leading to an elevation in the concentration of encapsulated chemicals specifically within the desired organ. The process of microbubble disintegration alters the permeability of capillaries, hence increasing the ability of blood vessels and tissues to allow the passage of chemicals that are meant to be delivered (Lu *et al.*, 2022).

In this investigation, the efficiency of ultrasound-targeted nanobubble destruction for the delivery of TAK-242 into the rat liver and kidney was evaluated, contingent on the duration of ultrasound exposure. The ultrasound was administered at a frequency of 5 MHz with an irradiation period of 15 minutes. The impact of ultrasound on TAK-242-loaded nanobubbles was comprehensively assessed through biochemical assays, gene expression analyses, and histopathological studies.

TLR4 presents a promising therapeutic target for patients with liver diseases due to its involvement in numerous inflammatory and fibrotic processes. It plays a crucial role in modulating the extent of liver fibrosis induced by various pathological conditions (Rivera *et al.*, 2007).

In the present study, our gene expression analysis revealed elevated TLR4 levels in the AFB1-exposed group, whereas TLR4 expression was markedly reduced following TAK-

242(downregulated 4.5-fold)-79.3 efficacy in treatment. The upregulation of TLR4 in hepatic and renal tissues associated with hepatorenal syndrome likely promotes the secretion of inflammatory mediators and ROS, which can be attributed to the enhanced permeability of blood vessels and intestines (Angeli *et al.*, 2019). The TLR4 signaling pathway has been identified as a critical target for reducing inflammation and alleviating hepatic and renal injuries in hepatorenal syndrome (Wang *et al.*, 2022).

Engelmann *et al.* established that TAK-242, a selective antagonist of the TLR4 receptor, mitigates the intensity of inflammation and hepatocyte apoptosis, hence enhancing organ functionality. The results clearly endorse the need for clinical trials of TAK-242, since it has the potential to improve liver failure and serve as a possible treatment for hepatic diseases by blocking TLR4 signaling (Engelmann *et al.*, 2020).

In the current study, rats exposed to AFB1 and treated concurrently with ultrasound nanobubbles loaded with TAK-242 exhibited significant improvements in serum biochemical parameters and reduced hepatic and renal histopathological alterations. These benefits can be attributed to the antioxidative, anti-inflammatory, and anticarcinogenic properties of TAK-242-loaded ultrasound nanobubbles, potentially due to their high phenolic and flavonoid content, which underscores their antioxidant effect .

TAK-242 enhances oxidative stress mitigation, mitochondrial function, and inflammatory response by inhibiting the TLR4/NF- $\kappa$ B signaling pathway (Xia *et al.*, 2024).

In a 2021 study conducted by Wen and Parikh, it was shown that the administration of TAK-242 resulted in a considerable reduction in the serum levels of blood urea nitrogen (BUN), creatinine (Cr), and cystatin C (Cys-C) in rats (Wen and Parikh, 2021). Previous research conducted by Wang *et al.* (Wang *et al.*, 2020) found that TAK-242 reduced serum markers of kidney injury and alleviated histological alterations in rats with crush injury-induced acute renal injury. In addition, Mohammad *et al.* demonstrated that TAK-242 has the ability to improve the typical characteristics of acute kidney damage (AKI) caused by ischemia/reperfusion, thereby offering protective benefits to the kidney (Mohammad *et al.*, 2018). In addition, Salama *et al.* (Salama *et al.*, 2015) Demonstrated that TAK-242 successfully averted renal failure. A study conducted by Sujie Liu and colleagues in 2022 revealed that TAK-242 has the ability to suppress the TLR4/NF- $\kappa$ B signaling pathway via the liver-gut axis. This mechanism effectively reduces the inflammatory response and provides relief from heart failure in rat models (Liu *et al.*, 2022).

Moreover, TAK-242 has demonstrated hepatoprotective properties in mouse models of lipopolysaccharide/D-galactose-induced fulminant hepatitis (Wang *et al.*, 2021). Additionally, it has proven effective in reducing TLR4 signaling to alleviate both acute and chronic liver failure in animals. TAK-242 has also been shown to decrease target organ damage and systemic inflammation in many animal models, including reducing ischemia/reperfusion injury in transplanted livers (Behzadi *et al.*, 2022).

The research conducted by Hu *et al.* (Hu *et al.*, 2020) And Liu *et al.* (Liu *et al.*, 2015) Has been revealed that the TLR4/MyD88/NF- $\kappa$ B signaling pathway may provide anti-inflammatory and hepatoprotective advantages by reducing the buildup of extracellular matrix (ECM) and inhibiting the production of pro-inflammatory substances. TLR4 plays a crucial role as the main detector for bacterial presence in the gastrointestinal tract and is a vital component of the innate immune system in the gut. It serves as both a receptor on the cell surface for immunological identification and as a signaling entity within the cell's membrane. Furthermore, the levels of TLR4 and NF- $\kappa$ B in the small intestines of rats with heart failure (HF) were significantly reduced after the administration of TAK-242. This indicates that the beneficial effects of TAK-242 in HF rats may be achieved by suppressing the inflammatory response driven by the TLR4/NF- $\kappa$ B pathway through the liver-gut connection.

NGAL, a protein predominantly found in neutrophils, stands as one of the most thoroughly investigated potential diagnostic biomarkers (Zhao *et al.*, 2010). It is esteemed as an exceedingly sensitive marker for renal injury, manifesting in both plasma and urine within two hours of injury—substantially preceding the elevation of sCr, which typically becomes apparent 24 to 48 hours post-insult (Francoz *et al.*, 2016).

The study found that the expression of the NGAL gene was reduced (5.1 fold) - 82.5% efficiency in the treated group compared to the group exposed to aflatoxin B1. Corroborating these discoveries, Mathias and Zahler *et al.* (Zahler *et al.*, 2022) Proposed that NGAL is indicative of both tubular damage and inflammatory reactions. According to Mathias *et al.* (2023), NGAL is an inflammatory biomarker that is linked to acute kidney damage (AKI). In addition, Shabnum Khawaja *et al.* (Khawaja *et al.*, 2019) Provided evidence that NGAL serves as an early and precise indicator for the prediction of AKI. It can serve as a biomarker to diagnose AKI early in critically ill patients with sepsis in the ICU, allowing for the start of potentially effective treatments before irreversible kidney damage takes place.

Previous studies have found a positive correlation between high levels of NGAL in the blood and the occurrence of AKI. NGAL is a promising biomarker for early prediction of AKI since it accumulates early and can be detected in circulation before creatinine. Although creatinine is now considered the most reliable method for promptly identifying kidney injury, NGAL's capacity to predict future AKI enables the prevention of kidney damage and enhances the overall prognosis (Albert *et al.*, 2021, Zou *et al.*, 2022).

Additionally, NGAL plays a crucial role in regulating cell proliferation, repair processes, and tubular re-epithelialization. Its expression is linked to an auxiliary iron transport pathway, which enhances the transcription of hemoxygenase—an enzyme that exerts proliferative and anti-apoptotic effects, thereby protecting and preserving proximal tubular cells (Mori *et al.*, 2005, Yang *et al.*, 2002).

The findings of this study offer new perspectives on the therapeutic potential of ultrasound nanobubbles loaded with TAK-242 to enhance localized drug delivery. By serving as both a carrier for TAK-242 and an ultrasound contrast agent, these nanobubbles facilitate targeted drug release. Upon ultrasound irradiation, they are selectively disrupted at specific sites, thereby improving the absorption efficiency of medications in areas affected by acute hepatorenal failure induced by aflatoxin B1.

### **Conclusion**

In conclusion, oral administration of aflatoxin B1 induced significant impairments in antioxidant defenses and hepatic and renal functions, accompanied by observable histopathological changes in the liver and kidney of rats. However, simultaneous administration of US nanobubbles loaded with TAK-242 alongside aflatoxin B1 mitigated these toxic effects. The beneficial impact of US nanobubbles loaded with TAK-242 is likely attributed to their antioxidative properties and ability to scavenge free radicals. Our findings suggest that employing US nanobubbles loaded with TAK-242 could potentially mitigate aflatoxin B1-induced hepatorenal toxicity. Future investigations should explore the efficacy of US nanobubbles loaded with TAK-242 against other environmental contaminants to further elucidate their therapeutic potential.

### **Declarations**

**Ethical Approval:** The study followed the ethical guidelines of Benha University, Faculty of Medicine.

**Competing Interests:** The authors declare no conflicts of interest.

**Authors' Contributions:** I hereby verify that all authors mentioned on the title page have made substantial contributions to the conception and design of the study, have thoroughly

reviewed the manuscript, confirm the accuracy and authenticity of the data and its interpretation, and consent to its submission.

**Funding:** No funding was received.

**Availability of Data and Materials:** All datasets analyzed and described during the present study are available from the corresponding author upon reasonable request.

**Acknowledgements:** DR Esam Rashwan ,VACSERA.,EGYPT

## REFERENCES

- Abdel-Aziem, S. H., Hassan, A. M., El-Denshary, E. S., Hamzawy, M. A., Mannaa, F. A. & Abdel-Wahhab, M. A. 2014. Ameliorative effects of thyme and calendula extracts alone or in combination against aflatoxins-induced oxidative stress and genotoxicity in rat liver. *Cytotechnology*, 66, 457-70.
- Abdel-Wahhab, M. A., Omara, E. A., Abdel-Galil, M. M., Hassan, N. S., Nada, S. A., Saeed, A. & El-Sayed, M. M. 2007. Zizyphus spina-christi extract protects against aflatoxin B1-initiated hepatic carcinogenicity. *African journal of traditional, complementary, and alternative medicines*, 4, 248-56.
- Aborehab, N. M. & Waly, N. E. 2019. IL-6 and NFE2L2: A putative role for the hepatoprotective effect of N. Sativa, P. Ginseng and C. Sempervirens in AFB-1 induced hepatocellular carcinoma in rats. *Toxicology reports*, 6, 457–464.
- Albert, C., Haase, M., Albert, A., Zapf, A., Braun-Dullaeus, R. C. & Haase-Fielitz, A. 2021. Biomarker-Guided Risk Assessment for Acute Kidney Injury: Time for Clinical Implementation? *Annals of laboratory medicine*, 41, 1-15.
- Angeli, P., Garcia-Tsao, G., Nadim, M. K. & Parikh, C. R. 2019. News in pathophysiology, definition and classification of hepatorenal syndrome: A step beyond the International Club of Ascites (ICA) consensus document. *J Hepatol*, 71, 811-822.
- Bancroft, J. D. & Gamble, M. 2008. *Theory and practice of histological techniques*, Elsevier health sciences.
- Batte, A., Menon, S., Ssenkusu, J. M., Kiguli, S., Kalyesubula, R., Lubega, J., Berrens, Z., Mutebi, E. I., Ogwang, R. & Opoka, R. O. 2022. Neutrophil gelatinase-associated lipocalin is elevated in children with acute kidney injury and sickle cell anemia, and predicts mortality. *Kidney international*, 102, 885-893.
- Behzadi, P., Sameer, A. S., Nissar, S., Banday, M. Z., Gajdacs, M., García-Perdomo, H. A., Akhtar, K., Pinheiro, M., Magnusson, P., Sarshar, M. & Ambrosi, C. 2022. The Interleukin-1 (IL-1) Superfamily Cytokines and Their Single Nucleotide Polymorphisms (SNPs). *Journal of immunology research*, 2022, 2054431.
- Bernabucci, U., Colavecchia, L., Danieli, P. P., Basiricò, L., Lacetera, N., Nardone, A. & Ronchi, B. 2011. Aflatoxin B1 and fumonisin B1 affect the oxidative status of bovine peripheral blood mononuclear cells. *Toxicology in vitro*, 25, 684-91.
- Chen, Z. Y., Wang, Y. X., Zhao, Y. Z., Yang, F., Liu, J. B., Lin, Y., Liao, J. Y., Liao, Y. Y. & Zhou, Q. L. 2014. Apoptosis induction by ultrasound and microbubble mediated drug delivery and gene therapy. *Current molecular medicine*, 14, 723-36.
- Choi, K. C., Chung, W. T., Kwon, J. K., Yu, J. Y., Jang, Y. S., Park, S. M., Lee, S. Y. & Lee, J. C. 2010. Inhibitory effects of quercetin on aflatoxin B1-induced hepatic damage in mice. *Food and chemical toxicology*, 48, 2747-53.
- Darwish, H., Omara, E., Abdel-Aziz, K., Farag, I., Nada, S. & Tawfek, N. 2011. Saccharomyces cerevisiae modulates Aflatoxin-induced toxicity in male Albino mice. *Report and Opinion*, 3, 32-43.

- Deng, Z. J., Zhao, J. F., Huang, F., Sun, G. L., Gao, W., Lu, L. & Xiao, Q. 2020. Protective Effect of Procyanidin B2 on Acute Liver Injury Induced by Aflatoxin B (1) in Rats. *Biomedical and environmental sciences*, 33, 238-247.
- El-Zayat, S. R., Sibaii ,H. & Mannaa, F. A. 2019. Toll-like receptors activation, signaling, and targeting: an overview. *Bulletin of the National Research Centre*, 43, 187.
- Embaby, E.-S. M., Ayaat, N. M., Abdel-Hameid, N.-A., Abdel-Galil, M. M., Mohamed, S. R. & Younos, M. A. 2015 .Effect of detoxification of aflatoxins by ozone or hot air on albino rats. *The Egyptian Journal of Experimental Biology (Zoology)*, 11, 107-115.
- Endo-Takahashi, Y. & Negishi, Y. 2020. Microbubbles and Nanobubbles with Ultrasound for Systemic Gene Delivery. *Pharmaceutics*, 12 (10):964.
- Engelmann, C., Sheikh, M., Sharma, S., Kondo, T., Loeffler-Wirth, H., Zheng, Y. B., Novelli, S., Hall, A., Kerbert, A. J. & Macnaughtan, J. 2020. Toll-like receptor 4 is a therapeutic target for prevention and treatment of liver failure. *Journal of hepatology*, 73, 102-112.
- Farag, M. R. & Alagawany, M. 2018. Erythrocytes as a biological model for screening of xenobiotics toxicity. *Chemico-biological interactions*, 279, 73-83.
- Feng, Y., Ju, Y., Wu, Q., Sun, G. & Yan, Z. 2023. TAK-242, a toll-like receptor 4 antagonist, against brain injury by alleviates autophagy and inflammation in rats. *Open life sciences*, 18, 20220662.
- Francoz, C., Nadim, M. K. & Durand, F. 2016. Kidney biomarkers in cirrhosis. *Journal of hepatology*, 65, 809-824.
- Guo, X.-M., Chen, J.-L., Zeng, B.-H., Lai, J.-C., Lin, C.-Y. & Lai, M.-Y. 2020. Ultrasound-mediated delivery of RGD-conjugated nanobubbles loaded with fingolimod and superparamagnetic iron oxide nanoparticles: targeting hepatocellular carcinoma and enhancing magnetic resonance imaging. *RSC advances*, 10, 39348-39358.
- Hendrayani, S. F., Al-Harbi, B., Al-Ansari, M. M., Silva, G. & Aboussekhra, A. 2016. The inflammatory/cancer-related IL-6/STAT3/NF- $\kappa$ B positive feedback loop includes AUF1 and maintains the active state of breast myofibroblasts. *Oncotarget*, 7, 41974-41985.
- Hu, N., Guo, C., Dai, X., Wang, C., Gong, L., Yu, L., Peng, C. & Li, Y. 2020. Forsythiae Fructuse water extract attenuates liver fibrosis via TLR4/MyD88/NF- $\kappa$ B and TGF- $\beta$ /smads signaling pathways. *Journal of ethnopharmacology*, 262, 113275.
- Kawai, T. & Akira, S. 2010. The role of pattern-recognition receptors in innate immunity: update on Toll-like receptors. *Nature immunology*, 11, 373-84.
- Kawamoto, T., Ii, M., Kitazaki, T., Iizawa, Y. & Kimura, H. 2008. TAK-242 selectively suppresses Toll-like receptor 4-signaling mediated by the intracellular domain. *European journal of pharmacology*, 584, 40-8.
- Khawaja, S., Jafri, L., Siddiqui, I., Hashmi, M. & Ghani, F. 2019. The utility of neutrophil gelatinase-associated Lipocalin (NGAL) as a marker of acute kidney injury) AKI) in critically ill patients. *Biomarker research*, 7, 4.
- Lawrence, T. 2009. The nuclear factor NF-kappaB pathway in inflammation. *Cold Spring Harbor perspectives in biology*, 1, a001651.
- Li, H., Xing, L., Zhang, M., Wang, J. & Zheng, N. 2018. The Toxic Effects of Aflatoxin B1 and Aflatoxin M1 on Kidney through Regulating L-Proline and Downstream Apoptosis. *BioMed research international*, 2018, 9074861.
- Liu, M., Xu, Y., Han, X., Yin, L., Xu, L., Qi, Y., Zhao, Y., Liu, K. & Peng, J. 2015. Dioscin alleviates alcoholic liver fibrosis by attenuating hepatic stellate cell activation via the TLR4/MyD88/NF- $\kappa$ B signaling pathway. *Scientific Reports*, 5, 18038.

- Liu, S., Wu, J., Chen, P., Mohammed, S. A. D., Zhang, J. & Liu, S. 2022. TAK-242 Ameliorates Hepatic Fibrosis by Regulating the Liver-Gut Axis. *BioMed research international*, 2022, 4949148.
- Lu, S., Zhao, P., Deng, Y. & Liu, Y. 2022. Mechanistic Insights and Therapeutic Delivery through Micro/Nanobubble-Assisted Ultrasound. *Pharmaceutics*, 14(3), 480.
- Matsunaga, N., Tsuchimori, N., Matsumoto, T. & Ii, M. 2011. TAK-242 (resatorvid), a small-molecule inhibitor of Toll-like receptor (TLR) 4 signaling, binds selectively to TLR4 and interferes with interactions between TLR4 and its adaptor molecules. *Molecular pharmacology*, 79, 34-41.
- Medina, A., Rodriguez, A. & Magan, N. 2014. Effect of climate change on *Aspergillus flavus* and aflatoxin B1 production. *Frontiers in microbiology*, 5, 348.
- MOHAMMAD, B. I., RAHEEM, A. K., HADI, N. R., JAMIL, D. A. & AL-AUBAIDY, H. A. 2018. Reno-protective effects of TAK-242 on acute kidney injury in a rat model. *Biochemical and biophysical research communications*, 503, 304-308.
- Mori, K., Lee, H. T., Rapoport, D., Drexler, I. R., Foster, K., Yang, J., Schmidt-Ott, K. M., Chen, X., Li, J. Y., Weiss, S., Mishra, J., Cheema, F. H., Markowitz, G., Suganami, T., Sawai, K., Mukoyama, M., Kunis, C., D'agati, V., Devarajan, P. & Barasch, J. 2005. Endocytic delivery of lipocalin-siderophore-iron complex rescues the kidney from ischemia-reperfusion injury. *The Journal of clinical investigation*, 115, 610-21.
- Mtimet, N., Walke, M., Baker, D., Lindahl, J., Hartmann, M. & Grace, D. 2015. Kenyan awareness of aflatoxin: An analysis of processed milk consumers. Poster presented at the 29th International Conference of Agricultural Economists (ICAE), Milan, Italy, 8-14 August 2015. Nairobi: ILRI.
- Nugraha, A., Khotimah, K. & Rietjens, I. 2018. Risk assessment of aflatoxin B1 exposure from maize and peanut consumption in Indonesia using the margin of exposure and liver cancer risk estimation approaches. *Food and chemical toxicology*, 113, 134-144.
- Park, J. H. & Park, I. Y. 2023. Effects of Ultrasound Targeted Destruction of Echogenic Nanobubbles Containing Doxorubicin in Rat Liver. *Journal of Surgical Ultrasound*, 10, 32-41.
- Peyman, S. A., McLaughlan, J. R., Abou-Saleh, R. H., Marston, G., Johnson, B. R., Freear, S., Coletta, P. L., Markham, A. F. & Evans, S. D. 2016. On-chip preparation of nanoscale contrast agents towards high-resolution ultrasound imaging. *Lab on a Chip*, 16, 679-687.
- Reda, F. M., Ismail, I. E., El-Mekkawy, M. M., Farag, M. R., Mahmoud, H. K. & Alagawany, M. 2020. Dietary supplementation of potassium sorbate, hydrated sodium calcium aluminosilicate and methionine enhances growth, antioxidant status and immunity in growing rabbits exposed to aflatoxin B1 in the diet. *Journal of animal physiology and animal nutrition*, 104, 196-203.
- Rivera, C. A., Adegboyega, P., Van Rooijen, N., Tagalicud, A., Allman, M. & Wallace, M. 2007. Toll-like receptor-4 signaling and Kupffer cells play pivotal roles in the pathogenesis of non-alcoholic steatohepatitis. *Journal of hepatology*, 47, 571-9.
- Rushing, B. R. & Selim, M. I. 2019. Aflatoxin B1: A review on metabolism, toxicity, occurrence in food, occupational exposure, and detoxification methods. *Food and chemical toxicology*, 124, 81-100.
- Salama, M., Elgamal, M., Abdelaziz, A., Ellithy, M., Magdy, D., Ali, L., Fekry, E., Mohsen, Z., Mostafa, M., Elgamal, H., Sheashaa, H. & Sobh, M. 2015. Toll-like receptor 4 blocker as potential therapy for acetaminophen-induced organ failure in mice. *Experimental and Therapeutic Medicine*, 10, 241-246.

- Shah, N., Mohamed, F. E., Jover-Cobos, M., Macnaughtan, J., Davies, N., Moreau, R., Paradis, V., Moore, K., Mookerjee, R. & Jalan, R. 2013. Increased renal expression and urinary excretion of TLR4 in acute kidney injury associated with cirrhosis. *Liver international*, 33, 398-409.
- Somorin, Y. M., Bertuzzi, T., Battilani, P. & Pietri, A. 2012. Aflatoxin and fumonisin contamination of yam flour from markets in Nigeria. *Food Control*, 25, 53-58.
- Sun, X., Guo, L., Shang, M., Shi, D., Liang, P., Jing, X., Meng, D., Liu, X., Zhou, X., Zhao, Y. & Li, J. 2020. Ultrasound Mediated Destruction of LMW-HA-Loaded and Folate-Conjugated Nanobubble for TAM Targeting and Reeducation. *International journal of nanomedicine*, 15, 1967-1981.
- Sun, Y., Park, I., Guo, J., Weaver, A. C. & Kim, S. W. 2015. Impacts of low level aflatoxin in feed and the use of modified yeast cell wall extract on growth and health of nursery pigs. *Animal nutrition*, 1, 177-183.
- Suzuki, R., Oda, Y., Omata, D., Nishiie, N., Koshima, R., Shiono, Y., Sawaguchi, Y., Unga, J., Naoi, T., Negishi, Y., Kawakami, S., Hashida, M. & Maruyama, K. 2016. Tumor growth suppression by the combination of nanobubbles and ultrasound. *Cancer science*, 107, 217-23.
- Tian, Y., Liu, Z., Zhang, L., Zhang, J., Han, X., Wang, Q & Cheng, W. 2018. Apatinib-loaded lipid nanobubbles combined with ultrasound-targeted nanobubble destruction for synergistic treatment of HepG2 cells in vitro. *OncoTargets and therapy*, 11, 4785-4795.
- Vázquez-Carballo, C., Guerrero-Hue, M., García-Caballero, C., Rayego-Mateos, S., Opazo-Ríos, L., Morgado-Pascual, J. L., Herencia-Bellido, C., Vallejo-Mudarra, M., Cortegano, I., Gaspar, M. L., De Andrés, B., Egido, J. & Moreno, J. A. 2021. Toll-Like Receptors in Acute Kidney Injury. *International journal of molecular sciences*, 22(2), 816.
- Wang, H., Li, X., Dong, G., Yan, F., Zhang, J., Shi, H., Ning, Z., Gao, M., Cheng, D., Ma, Q., Wang, C., Zhao, M., Dai, J., Li, C., Li, Z., Zhang, H. & Xiong, H. 2021. Toll-like Receptor 4 Inhibitor TAK-242 Improves Fulminant Hepatitis by Regulating Accumulation of Myeloid-Derived Suppressor Cell. *Inflammation*, 44, 671-681.
- Wang, J., Chen, Z., Hou, S., Liu, Z. & Lv, Q. 2020. TAK-242 Attenuates Crush Injury Induced Acute Kidney Injury through Inhibiting TLR4/NF- $\kappa$ B Signaling Pathways in Rats. *Prehospital and disaster medicine*, 35(6), 619-628.
- Wang, M., Qin, T., Zhang, Y., Zhang, T., Zhuang, Z., Wang, Y., Ding, Y. & Peng, Y. 2022. Toll-like receptor 4 signaling pathway mediates both liver and kidney injuries in mice with hepatorenal syndrome. *American journal of physiology. Gastrointestinal and liver physiology*, 323(5), G461-G476.
- Wen, Y. & Parikh, C. R. 2021. Current concepts and advances in biomarkers of acute kidney injury. *Critical reviews in clinical laboratory sciences*, 58, 354-368.
- Xia, Y. M., Guan, Y. Q., Liang, J. F. & Wu, W. D. 2024. TAK-242 improves sepsis-associated acute kidney injury in rats by inhibiting the TLR4/NF- $\kappa$ B signaling pathway. *Renal failure*, 46, 2313176.
- Yang, J., Goetz, D., Li, J. Y., Wang, W., Mori, K., Setlik, D., Du, T., Erdjument-Bromage, H., Tempst, P., Strong, R. & Barasch, J. 2002. An iron delivery pathway mediated by a lipocalin. *Molecular cell*, 10, 1045-56.
- Zahler, D., Merdler, I., Banai, A., Shusterman, E., Feder, O., Itach, T., Robb, L., Banai, S. & Shacham, Y. 2022. Predictive Value of Elevated Neutrophil Gelatinase-Associated Lipocalin (NGAL) Levels for Assessment of Cardio-Renal Interactions among ST-Segment Elevation Myocardial Infarction Patients. *Journal of clinical medicine*, 11(8), 2162.

- Zhang, J., Wei, L. & Zhao, Y. 2020. Synthesis of nanobubbles for improved ultrasound tumor-imaging applications. *3 Biotech*, 10, 12.
- Zhang, Y.-L., Qiao ,S.-K., Wang, R.-Y. & Guo, X.-N. 2018. NGAL attenuates renal ischemia/reperfusion injury through autophagy activation and apoptosis inhibition in rats. *Chemico-biological interactions*, 289, 40-46.
- Zhao, C., Ozaeta, P., Fishpaugh, J., Rupprecht, K., Workman, R., Grenier, F. & Ramsay, C. 2010. Structural characterization of glycoprotein NGAL, an early predictive biomarker for acute kidney injury. *Carbohydrate research*, 345, 2252-2261.
- Zhong, X., Xiao, Q., Liu, Z., Wang, W., Lai, C. H., Yang, W., Yue, P., Ye ,Q. & Xiao, J. 2019. TAK242 suppresses the TLR4 signaling pathway and ameliorates DCD liver IRI in rats. *Molecular medicine reports*, 20, 2101-2110.
- Zou, C., Wang, C. & Lu, L. 2022. Advances in the study of subclinical AKI biomarkers. *Frontiers in physiology*, 13, 960059

### ARABIC SUMMARY

نظرة ثاقبة حول التأثير العلاجي للفقاعات النانوية بالموجات فوق الصوتية المحملة بـ TAK-242 على السمية الكبدية الكلوية المستحثة بالأفلاتوكسين B1 في الجرذان

سحر محمد ابوالوفا<sup>1</sup> - سنيه خيرى عليوة<sup>2</sup> - سالي الشرقاوي<sup>1</sup>

1- قسم الطب الشرعي والسموم الاكلينيكية - كلية الطب البشري - جامعة بنها - مصر  
2- قسم الكيمياء الحيوية والبيولوجيا الجزيئية - كلية الطب البشري - جامعة بنها - مصر

الأفلاتوكسين ب 1 هو عامل جينوتوكسين قوي ومسرطن للكبد، مما يشكل خطراً كبيراً على الصحة العامة. هدفت هذه الدراسة إلى تقييم ما إذا كانت الفقاعات النانوية المحملة بعقار TAK-242 يمكن أن تخفف من سمية الكبد والكلية الناتجة عن الأفلاتوكسين ب 1 في الفئران. تم تقسيم اثنين وثلاثين فأراً أبيضاً ذكراً إلى أربع مجموعات: مجموعة ضابطة، مجموعة تتلقى فقاعات نانوية محملة بعقار TAK-242، مجموعة تتغذى على الأفلاتوكسين ب 1، ومجموعة تتغذى على الأفلاتوكسين ب 1 وتعالج بفقاعات نانوية محملة بعقار TAK-242. شملت المعالجة حقن 150 ميكرو لتر من الفقاعات النانوية كل يومين بعد تناول الأفلاتوكسين ب 1، مع دمجها بـ 15 دقيقة من الموجات فوق الصوتية (5 ميغاهرتز). بعد 14 يوماً، تم إجراء القياسات البيوكيميائية، التعبير الجيني، والفحوصات النسيجية. أظهرت الفئران المسممة بالأفلاتوكسين ب 1 انخفاضاً في مستويات الجلوتاثيون، والسوبر أكسيد ديسموتاز، والكاتالاز في البلازما، مع زيادة في المالونديالديهايد، والإنترلوكين 6، وعامل نخر الورم ألفا، والآنين أمينوترانسفيراز، وأسبارتات أمينوترانسفيراز، والفوسفاتاز القلوي، واليوريا، ومستويات الكرياتينين، وزيادة في التعبير الجيني لمستقبلات تول الشبيهة 4 والبروتين الدهني المرتبط بجيلاتيناز العدلات، بجانب تلف كبير في أنسجة الكبد والكلية. عالجت الفقاعات النانوية المحملة بعقار TAK-242 بشكل كبير هذه التأثيرات السامة، مما حسن من الحالة المضادة للأكسدة وقلل من التغيرات البيوكيميائية والنسيجية في الكبد والكلية.